RSC Advances

PAPER

View Article Online
View Journal | View Issue

Cite this: *RSC Adv.*, 2017, **7**, 44751

Adsorption of Cu(II) ions in aqueous solution by aminated lignin from enzymatic hydrolysis residues

Jun Xu,[ab] Shiyun Zhu,[a] Peng Liu,[a] Wenhua Gao,[a] Jun Li*[a] and Lihuan Mo[a]

Aminated lignin (AL) has been prepared by a Mannich reaction for the removal of Cu(II) ions from aqueous solution. Effects of pH, reaction temperature, reaction time and the initial concentration of Cu(II) ions on the adsorption capacity were investigated. The structure and properties of AL were analyzed by Fourier transform infrared spectroscopy (FT-IR), scanning electron microscopy analysis (SEM), and X-ray photoelectron spectroscopy analysis (XPS). Adsorption kinetic and isotherm models were used to illustrate the adsorption behaviors of AL. AL was more effective than enzymatic hydrolysis residues (EHR) and separated lignin (SL) in removing Cu(II) ions in aqueous solution. The adsorption capacity of AL for Cu(II) ions was better in near-neutral pH. Under the optimum adsorption conditions, the adsorption capacity of AL could reach up to 37.14 mg g^{-1}. The pseudo-second-order model fitted the kinetic data well. The adsorption isotherm was well described by the Langmuir isotherm model. AL exhibited a good adsorption performance for recovery after three cycles. AL could be utilized as a kind of promising feedstock for high value-added products to remove Cu(II) ions in wastewater effectively.

Received 15th June 2017
Accepted 6th September 2017

DOI: 10.1039/c7ra06693g

rsc.li/rsc-advances

1. Introduction

Cellulosic ethanol from lignocellulosic biomass like corn stalks, which are abundant and renewable resources, is considered as a feasible replacement of fossil fuel for transportation. The processing of cellulosic ethanol includes mechanical pretreatment, enzymatic hydrolysis and fermentation.[1] Therefore, EHR are produced as by-products simultaneously, which are mainly used as low-grade fuel to recover part of the energy cost but cause certain pollution to the environment.[2]

In addition, heavy metal ions have been excessively released into the environment due to rapid industrialization, which created a major global concern.[3] Heavy metal ions are typical contaminants which generate serious problems to all bodies from the aqueous medium as they are bio-accumulative and non-biodegradable.[4] Current techniques for the removal of toxic metals from an aqueous system have been developed for a long period, such as ion exchange,[5,6] membrane separation, reverse osmosis, ultrafiltration, electrodeposition[7] complexation precipitation, and biosorption.[8] Specially, biosorption is a higher effective, environmentally friendly, cheap, and easy way to operate comparing with other treatment processes.[9] AL as an excellent biosorbent for removal heavy metals has an attractive potential.

Biosorbents have the advantages of biocompatibility and biodegradability,[10] such as starch, chitosan,[11] cellulose, lignin and so on. EHR is considered as waste in the cellulosic ethanol industry,[12–14] which contains a lot of lignin and little of cellulose, hemicellulose and other impurities. Lignin is the main component in EHR and still retains its original chemical structure,[15] which could be separated from these residues and then modified as aminated lignin by Mannich reaction.[16] AL contains large amounts of reactive sites[17] such as amino group and phenolic hydroxyl,[18] and can be utilized as adsorbent to uptake heavy mental ions such as Cu(II) ions.[19–21] It is an eco-friendly and cost-effective method to make full use of aminated lignin to adsorb Cu(II) ions from aqueous solution.[22,23]

In one study, the alkali lignin from the black liquor of a kraft pulp mill was aminated with hexane-diamine to be a flocculant with ultrasonic assistance. It's more difficult to separate lignin from black liquor than from enzymatic hydrolysis residues, and its adsorption needs more assistance. In another study, aminated bagasse pith was reported as an ions adsorbent to remove copper(II) from aqueous solution, but the adsorption capacity of aminated bagasse pith was lower than some sorbents.[24]

The aim of this study was to carry out a thoroughly investigation of the adsorption of Cu(II) ions by AL from EHR,[25] including the adsorption kinetic, adsorption isotherm[26] and factors which could make a difference to the adsorption of Cu(II) ions onto AL such as pH, reaction temperature, reaction time and initial concentration of Cu(II) ions.[27] The relationship between the adsorption capacity and adsorption mechanisms was studied by Langmuir and Freundlich isotherms models.[28,29] Lignin from EHR of corn stalks in cellulosic ethanol process could be modified and then used to remove heavy metal ions which can maximize the economic value of the residues.

[a]*State Key Laboratory of Pulp and Paper Engineer, South China University of Technology, Guangzhou, Guangdong, 510640, China. E-mail: ppjunli@scut.edu.cn*
[b]*Key Laboratory of Pulp and Paper Science & Technology of Ministry of Education of China, Qilu University of Technology, Jinan, Shandong, 250353, China*

2. Materials and methods

2.1 Materials

EHR of corn stalk was obtained from a factory (Heilongjiang Province, China). Copper sulfate pentahydrate ($CuSO_4 \cdot 5H_2O$), epichlorohydrin and diethylenetriamine (DETA) were purchased from Runjie Chemical Reagent Co., Ltd. (Shanghai, China). Concentrated hydrochloric acid, nitric acid and sodium hydroxide were purchased from Kemiou Chemical Reagent Co., Ltd. (Tianjin, China). All other reagents were of analytical grade. The raw material was grinded to 100 mesh particles for further analysis.

2.2 Preparation of AL from EHR

The air-dried EHR particles were added into 40 g L^{-1} of NaOH solution (1 : 30, w/v) and soaked for 2.5 h at 60 °C in the water bath. After that, the mixture was filtrated and diluted HCl was used to adjust the pH value to 1.5, then the precipitation was centrifuged after standing for 12 hours at room temperature. The precipitation was washed with deionized water and filtrated then freeze-dried into SL.

The pre-weighted SL was mixed with 16.7% NaOH solution (1 : 10, w/v) and epichlorohydrin (1 : 10, w/v), and the mixture was agitated and heated at 80 °C for 3 hours, then 95.0% ethanol and deionized water was used to wash the product to neutral. The light yellow powdered epoxy lignin could be gained by freeze drying method from the product. After that, single factor experiments were applied to determine the optimum conditions for the synthesis of AL by a Mannich reaction. The factors and levels are showed in Table 1. 1.0 g epoxy lignin and 16.7% NaOH solution were added into a three-necked flask. This mixture was continuously stirred under temperature and time in Table 1. Then AL was washed, filtrated and dried by freeze drying again. The content of nitrogen element was used to determine the grafting of DETA onto epoxy lignin.

2.3 Characteristics of EHR, SL and AL

FT-IR spectra of EHR, SL and AL were recorded by Vector 33 type infrared spectrometer (Bruker, German). The element contents were measured by Vario EL cube element analyzer (Elementar, German). The appearance of EHR and AL were detected by EVO18 type SEM (Zeiss, German). The Cu(II) ions concentration was measured by the ZEEnit 700p flame graphite furnace atomic absorption spectrometer (F/GF-AAS) (Analytik Jena, German). The binding energy of AL was determined by the Axis Ultra DLD clutches multi-function XPS (Kratos, British).

Table 1 Conditions of signal factor experiment

	Level				
Factor	1	2	3	4	5
16.7% NaOH (mL)	10	20	30	40	50
DETA (mL)	10	20	30	40	50
Time (h)	2	3	4	5	6
Temperature (°C)	40	50	60	70	80

2.4 Adsorption procedure

Cu^{2+} solutions were prepared by dissolving $CuSO_4 \cdot 5H_2O$ in deionized water to reach a concentration of 100 mg L^{-1}. Diluted HCl (0.01 M) and NaOH (0.01 M) were dropped into Cu^{2+} solutions to adjust systemic pH value to 3.0, 3.5, 4.0, 4.5, 5.0, and 5.5, respectively. Batch experiments were carried out (at 25 °C) by agitating 100 mg of AL in 50 mL of Cu^{2+} solution (100 mg L^{-1}) for 150 min at 20, 30, 40, 50, and 60 °C, respectively. After that the Cu^{2+} concentration in the mixture was determined by F/GF-AAS, and the adsorption capacity of AL at adsorption equilibrium, q_e (mg g^{-1}), was calculated according to the following equation:

$$q_e = \frac{(C_0 - C_e)}{M} V \quad (1)$$

where C_0 and C_e are the initial and final concentration of Cu^{2+} in solution (mg L^{-1}), respectively. V is the volume of aqueous solution (mL), and M is the total mass of AL (g).

2.5 Adsorption kinetics analysis

The adsorption kinetics analysis was conducted with the following conditions: 100 mg of AL were added into 50 mL of Cu^{2+} solution (100 mg L^{-1}), and the mixture was agitated continuously for 5–360 min (200 rpm) at an optimum pH value and reaction temperature obtained from Section 2.4. The adsorption capacity of AL was calculated according to eqn (1). Pseudo-first-order and pseudo-second-order kinetic models were used to fit the adsorption kinetic data.

The pseudo-first-order kinetic equation is

$$\frac{dq_t}{dt} = k_1(q_e - q_t)$$

Which has a linear form of

$$\ln(q_e - q_t) = \ln q_e - k_1 t$$

The pseudo-second-order kinetic equation is

$$\frac{dq_t}{dt} = k_2(q_e - q_t)^2$$

which has a linear form of

$$\frac{t}{q_t} = \frac{1}{k_2 q_e^2} + \frac{t}{q_e}$$

where q_t (mg g^{-1}) is the adsorption capacity at time t (min), q_e (mg g^{-1}) is the adsorption capacity at adsorption equilibrium, and k_1 (min^{-1}) and k_2 (g mg^{-1} min^{-1}) are the kinetics rate constants for the pseudo-first-order and pseudo-second-order models, respectively.

2.6 Adsorption isotherms analysis

Adsorption isotherm analysis can describe the adsorption mechanism at equilibrium well.[29] The effect of the initial Cu^{2+} concentration on the adsorption capacity was investigated by variation of the initial concentration of Cu^{2+} at an optimum pH

value, reaction temperature and time. A total of 100 mg of AL was added into 50 mL of Cu^{2+} solution (50–300 mg L^{-1}) at appropriate conditions as above. At the end of this experiment, the adsorption capacity of AL was calculated according to eqn (1). Langmuir and Freundlich adsorption isotherm models were used to fit the adsorption isotherm data.

The Langmuir adsorption isotherm equation is

$$\frac{C_e}{q_e} = \frac{C_e}{q_f} + \frac{1}{q_f K_L}$$

The Freundlich adsorption isotherm equation is

$$\ln q_e = \ln K_F + \frac{\ln C_e}{n}$$

where q_e and C_e are the adsorption amount (mg g^{-1}) and concentration of metal ions in solution (mg L^{-1}) at equilibrium, respectively. K_L is the Langmuir constant (L mg^{-1}), and q_f is the maximum adsorption capacity of Cu^{2+} (mg g^{-1}). K_F and n are the Freundlich isotherm constants, indicating the adsorption capacity (mg g^{-1}) and adsorption intensity (dimensionless), respectively.

2.7 Contrast experiment and regeneration

Batch experiments were carried out (at 25 °C) by agitating 100 mg of AL, SL and EHR in 50 mL of Cu^{2+} solution under optimum conditions from 2.4, 2.5 and 2.6 respectively. Then the Cu^{2+} concentration was determined by F/GF-AAS. Three adsorbents were filtrated and washed with deionized water 3 times. Then, three adsorbents were added into HNO_3 solution (0.05 M) for 2 h under stirring to remove Cu^{2+}, then filtrated and washed with deionized water again. Finally, three recycled adsorbents were used to adsorb copper ion and the adsorption–desorption process was repeated 3 times. The adsorption capacity of adsorbents was calculated according to the eqn (1).

3. Results and discussion

3.1 Single factor experiment

The grafting ratio of AL depends on the nitrogen content. A higher nitrogen content indicates a better grafting modification. Results in Fig. 1 exhibited that AL could be well prepared by mixing epoxy lignin with 16.7% NaOH solution (1 : 30, w/v) and DETA (1 : 30, w/v) for 4 hours at 50 °C.

3.2 The FT-IR spectra analysis

The FT-IR spectra obtained from EHR, SL and AL were shown in Fig. 2 and 3. Absorption peak at 1654 cm^{-1} indicated aromatic ring of conjugated C=O stretching vibration.[14] Two absorption peaks at 1508 cm^{-1} and 1419 cm^{-1} could be assigned to typical aromatic skeleton vibrations.[14] The peaks at 1335 cm^{-1} was syringyl ring C–O stretching vibration and peaks at 1032 cm^{-1} indicated guaiacyl units.[30]

Comparing with the FT-IR spectra of AL and SL, the peaks of AL at 832 cm^{-1} of epoxy groups weakened significantly.[13] The peaks of AL at 1124 cm^{-1} of aliphatic C–N stretching vibration,

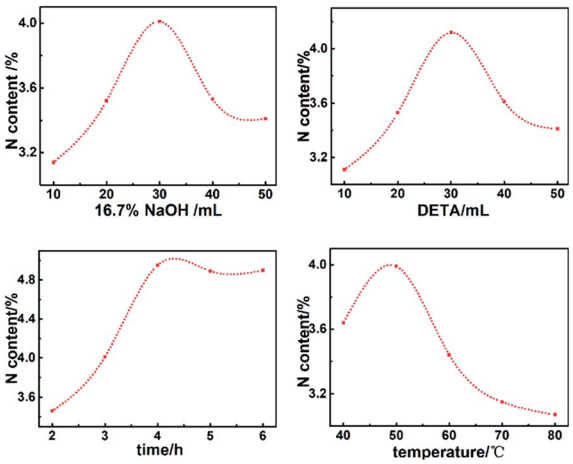

Fig. 1 Conditions of signal factor experiment.

1593 cm^{-1} of N–H swing vibration enhanced.[15] The broad band at 3400 cm^{-1} was dominated by the stretching vibrations of –OH groups.[11] These peaks indicated the presence of amino groups in AL, indicating that diethylenetriamine monomers could be grafted onto SL.[23,31,32]

3.3 SEM and XPS spectra analysis

Fig. 4(a) and (b) depicted the morphological changes of EHR and AL prior to the adsorption in Cu^{2+} solutions. EHR exhibited a macroporous structure. However, the surface of AL looked smoother than that of EHR. After modification, the expanded macropores gradually shrank and even flattened, and no apparent pores could be observed on the surface of AL.[23] The morphologies of Cu^{2+} adsorbed onto EHR and AL were also shown in Fig. 4(c) and (d). It could be observed that many irregular pieces appeared on the surface of both EHR and AL, which were the metal Cu salts.[10] Interestingly, the metal Cu salts adsorbed onto AL were more than EHR. Therefore, it could be concluded that plenty of active sites located on AL, and played an important role in Cu^{2+} adsorption.[10,33]

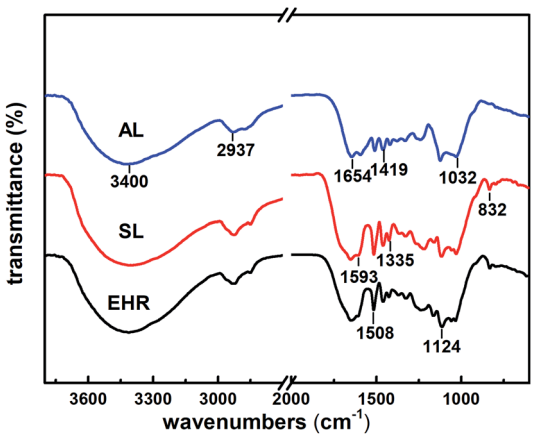

Fig. 2 FT-IR spectrum of AL, SL and EHR at wavenumbers 3800–800 cm^{-1}.

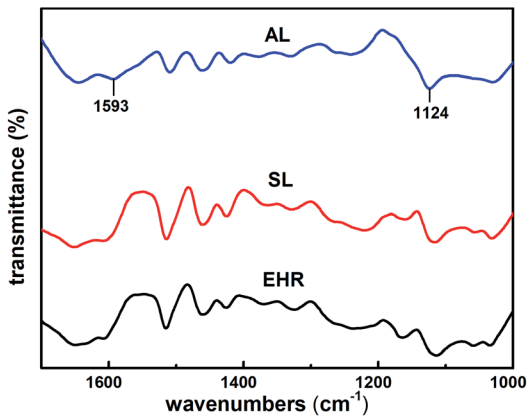

Fig. 3 Partial zoom in FT-IR spectrum of AL, SL and EHR at wavenumbers 1800–800 cm^{-1}.

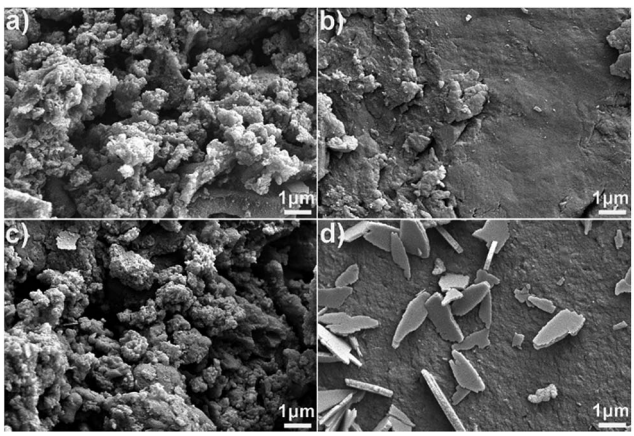

Fig. 4 Typical SEM micrographs: (a) EHR before Cu^{2+} adsorption, (b) AL before Cu^{2+} adsorption, (c) EHR after Cu^{2+} adsorption, (d) AL after Cu^{2+} adsorption.

Table 2 Element contents of EHR, SL and AL

	Element mass (%)		
Samples	Nitrogen	Carbon	Hydrogen
EHR	0.87	44.14	5.18
SL	1.03	42.04	4.71
AL	3.94	47.53	6.50

In order to make further research on the Cu^{2+} adsorption of AL, the Kratos Axis Ultra (DLD) type photoelectron spectrometer was used for chemical analysis of surface of AL. As shown in Fig. 5(a) and (d), there were no obvious changes before and after Cu^{2+} adsorption. As shown in Fig. 5(b), the peaks at binding energy of 399.8 eV and 401.1 eV respectively referred to $-NH_2$ groups and C-bonded CH_2CN ($-CH_2CN$), indicating that diethylenetriamine monomers could be grafted onto SL again.[34] Interestingly, it could be clearly found that the peak at binding energy of 397.5 eV appeared after Cu(II) ions adsorption in Fig. 5(e). It could be Cu–N bonds but hard to confirm whether Cu–N bonds exist or not. Thus, copper nitrides were not taken into consideration.[35] Meanwhile, Cu2p spectrum changed obviously comparing Fig. 5(c) with (f). There were five groups of peaks in Fig. 5(f). The peaks at binding energy of 940 eV and 947 eV represented $Cu2p_{2/3}$ spectra, indicating the Cu and N connection.[36] The point of 960 eV could be the characteristic peak of $Cu3d_{3/2}$. According to the ligand field theory, d orbital of Cu was incompletely filled and had strong coordination ability. Similarly, p orbital of N was incompletely filled, allowing reactions between Cu and N. In addition, $Cu2p_{1/2}$ at 952 eV and $Cu2p_{3/2}$ at 932 eV were observed and corresponded, respectively.[37] These results indicated that Cu^{2+} were adsorbed onto AL, which was consistent with SEM analysis.[34]

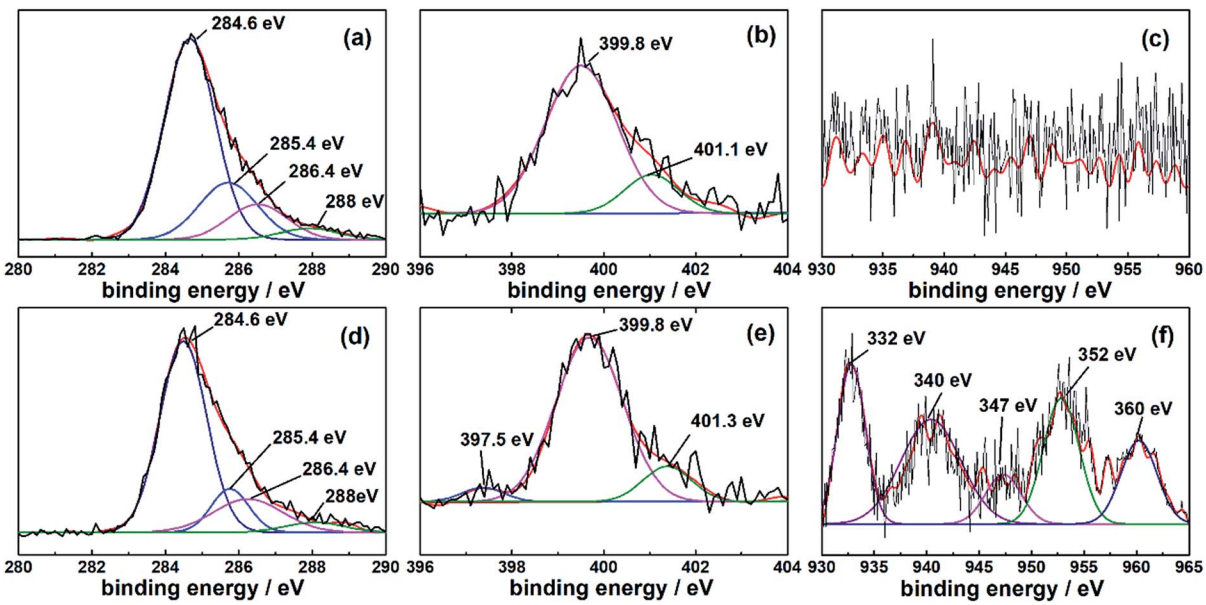

Fig. 5 Partial scan of AL before Cu^{2+} adsorption: (a) C1s, (b) N1s, (c) Cu2p; partial scan of AL after Cu^{2+} adsorption: (d) C1s, (e) N1s, (f) Cu2p.

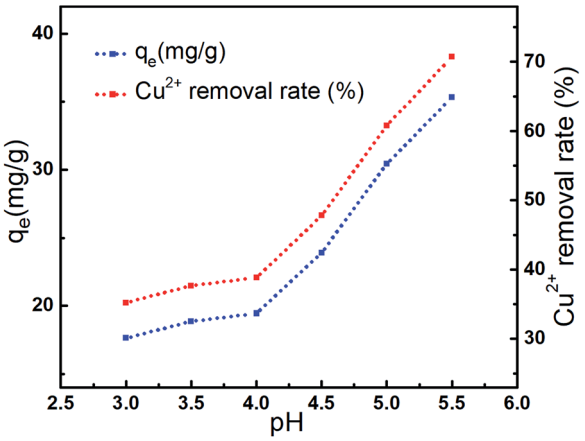

Fig. 6 Effect of the pH on the adsorption of Cu^{2+} onto AL.

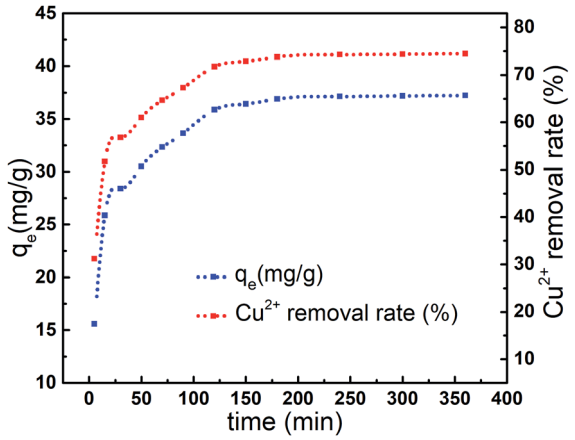

Fig. 8 Effect of time on the adsorption of Cu^{2+} onto AL at pH 5.5.

3.4 Elements analysis

The nitrogen element content in AL shown in Table 2 was as high as 3.94%, which increased by 282.5% compared to SL (1.03%), indicating that diethylenetriamine monomers could be grafted onto the lignin after two-step modification.[15,32] It was consistent with results of FT-IR spectra analysis.

3.5 Effect of the pH of Cu^{2+} solution on Cu^{2+} adsorptione

The effect of the pH on the metal ion adsorption capacity of AL was shown in Fig. 6. Results indicated that Cu^{2+} adsorption was strongly pH-dependent.[14] The adsorption capacity enhanced slightly when pH value ranged from 3 to 4, because the H^+ could make the active functional groups such as $-NH_2$ and $-O^-$ protonated, weakened the Cu^{2+} adsorption process, decreased the Cu^{2+} adsorption capacity.[23] When pH value increased from 4 to 5.5, the adsorption capacity of AL remarkably raised from 19.43 mg g^{-1} to 35.36 mg g^{-1}, and Cu^{2+} removal rate increased from 38.86% to 70.71%. The pH-dependence[11] of adsorption suggested that Cu^{2+} were adsorbed according to the ion-exchange mechanism.[23,25] These results indicated that aqueous solution system with pH 5.5 was the optimal condition.[31]

3.6 Effect of the reaction temperature on Cu^{2+} adsorption

As illustrated in Fig. 7, the adsorption capacity of Cu^{2+} onto AL increased 4.84%, and Cu^{2+} removal rate increased 9.68% when the temperature raised from 20 °C to 40 °C. However, the adsorption capacity and Cu^{2+} removal rate increased slowly in the range of 40–60 °C. It could be due to the fact that the interaction between Cu^{2+} and active groups such as hydroxyl and amino groups of AL was weaker at high temperatures.[10] Apparently, high reaction temperature indicated the enhancement of the adsorption capacity of Cu^{2+}.[15] The results indicated that the adsorption was endothermic in nature and mainly by chemisorption rather than physisorption.[18]

3.7 Adsorption kinetics and isotherms

The adsorption capacity of Cu^{2+} onto AL was investigated by a batch equilibrium technique for reaction time varying between 5 min and 360 min. Results was showed in Fig. 8, the adsorption capacity of Cu^{2+} onto AL raised from 15.59 mg g^{-1} to 37.14 mg g^{-1} when reaction time increased from 5 min to 240 min. However, the adsorption capacity slowed down after

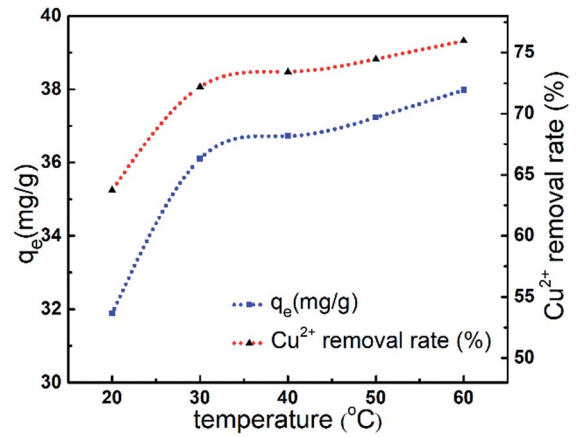

Fig. 7 Effect of the reaction temperature on the adsorption.

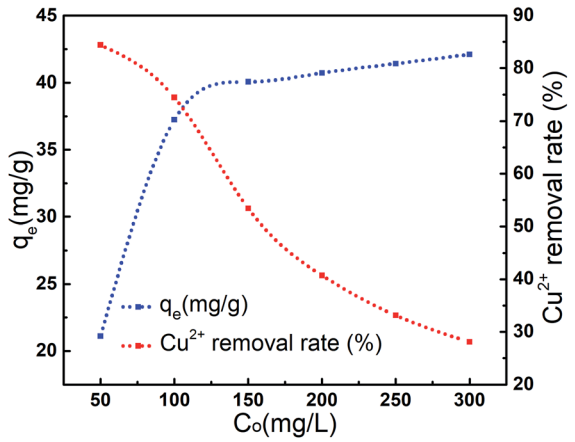

Fig. 9 Effect of the initial concentration on the adsorption of Cu^{2+} onto AL at pH 5.5.

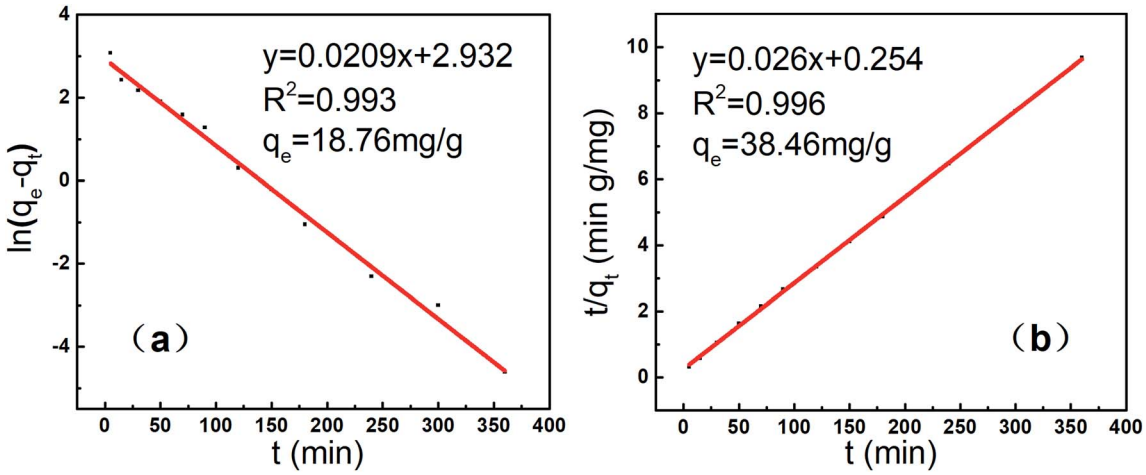

Fig. 10 Linear fitting curves of pseudo-first-order (a) and pseudo-second-order (b) kinetic models.

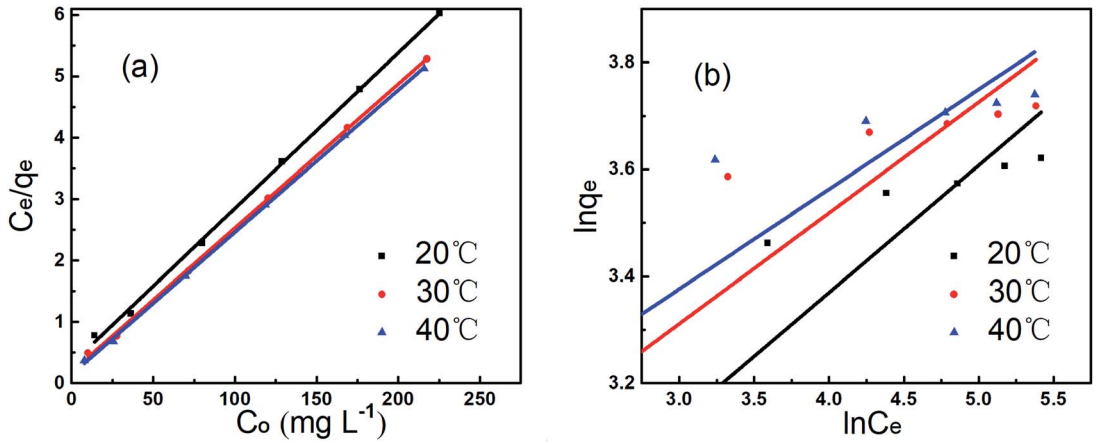

Fig. 11 Linear fitting curves of Langmuir (a) and Freundlich (b) isotherm models.

240 min. Results indicated that adsorption equilibrium could be achieved within 240 min.[15,23] The spontaneously high rate of Cu^{2+} uptake at short reaction time was associated with initial large number of vacant surface active sites available on AL.[18] Afterward the filling of vacant sites became difficult due to repulsive forces between Cu^{2+} adsorbed on AL surface and Cu^{2+} from solution.[29]

The effect of initial concentration of Cu^{2+} on the adsorption was illustrated in Fig. 9. The adsorption capacity increased sharply to 37.14 mg g^{-1} (at 100 mg L^{-1}) with the increase of initial concentration of Cu^{2+}, and adsorption equilibrium could be achieved.[10] At low concentration, the ratio of available binding sites to the total Cu^{2+} was high and Cu^{2+} could be bound to the active sites of AL.[15] Whereas, at high concentration, the ratio was lower and consequently binding sites were dependent on the initial concentration.[23]

On the basis of the time profiles above-mentioned, the pseudo-first-order and pseudo-second-order kinetic models were fitted and set up in Fig. 10. Clearly, the correlation coefficients R^2 for the pseudo-second-order kinetic model was higher and closer to 1 than those of the pseudo-first-order kinetic model, and the equilibrium adsorption quantity were closer to the experimental value from the pseudo-second-order kinetic model,[4] indicating that this adsorption system was a pseudo-second-order kinetic adsorption process.[10]

Experimental data were fitted to the Langmuir and Freundlich isotherm models as illustrated in Fig. 11, and parameters were presented in Table 3. Langmuir isotherm model fitted the experimental equilibrium data reasonably well with high correlation coefficients (R^2 > 0.99 at 40 °C). However, results of

Table 3 Linear equations parameters in the adsorption isotherm study of Cu^{2+} onto AL

Temperature (°C)	Langmuir isotherm			Freundlich isotherm		
	R^2	q_f (mg g^{-1})	K_L	R^2	n	K_F
20	0.9988	39.47	0.0802	0.7997	4.2017	11.22
30	0.9993	42.66	0.1260	0.7680	4.8277	14.73
40	0.9996	43.18	0.1602	0.7858	5.3022	16.71

Table 4 Adsorption capacity and regeneration of AL, SL and EHR

	Cycle 0	Cycle 1		Cycle 2		Cycle 3	
Adsorbents	q_e (mg g^{-1})	q_e (mg g^{-1})	R (%)	q_e (mg g^{-1})	R (%)	q_e (mg g^{-1})	R (%)
AL	37.22	36.15	97.12	35.37	95.03	32.57	87.51
SL	23.50	21.78	92.68	19.55	83.19	16.27	74.70
EHR	10.93	9.81	89.75	9.12	83.44	7.84	71.73

Freundlich isotherm model were not desirable with smaller R^2 values between 0.7858 and 0.7997. The $q_{f,cal}$ values calculated from the Langmuir isotherm model were close to the experimental data $q_{f,exp}$.[23] Therefore, Langmuir isotherm model provided the better fit for experimental data of AL, and could describe the adsorption of Cu^{2+} onto AL.[18]

3.8 Control experiment and regeneration

Table 4 exhibited that the adsorption capacity of AL, SL and EHR were 37.22, 23.50 and 10.93 mg g^{-1}, respectively, without regeneration. Additionally, the recovery efficiency of AL was high up to 87.51%, larger than that of SL and EHR in the third cycle. Results presented that AL had a better performance than SL and EHR in the adsorption capacity and regeneration.

4. Conclusion

Amino group can be grafted onto lignin separated from cellulosic ethanol enzymolysis residues well with epoxidation and amination modification. Aminated lignin put up a good performance for the removal of the metal Cu^{2+} with an efficient and environmentally friendly approach.

In addition, the adsorption kinetic has been studied and fitted the pseudo-second-order kinetic model well. Adsorption mechanism is consistent with the experimental data of Langmuir isotherm model. Under the optimum adsorption conditions, aminated lignin exhibits a good property that adsorption capacity could reach up to 37.14 mg g^{-1}. In summary, aminated lignin from cellulosic ethanol enzymolysis residue in consideration of their abundant supply makes them a potential and promising material for heavy metal ions removal for water treatment industries in the future.

Conflicts of interest

There are no conflicts to declare.

Acknowledgements

We gratefully acknowledge the financial support from the Special Support Plan of Guangdong Province (2014TQ01N603), Key Laboratory of Pulp and Paper Science & Technology of Ministry of Education of China (KF201508), Science & technology plan projects of Guangdong province (2015B020241001) and National Major Science and Technology Program for Water Pollution Control and Treatment (2014ZX07213).

References

1 C. H. Lai, M. B. Tu, Q. Yong and S. Y. Yu, *RSC Adv.*, 2015, **5**, 97966–97974.
2 D. Sud, G. Mahajan and M. P. Kaur, *Bioresour. Technol.*, 2008, **99**, 6017–6027.
3 H. N. M. Ekramul Mahmud, A. K. O. Huq and R. B. Yahya, *RSC Adv.*, 2016, **6**, 14778–14791.
4 A. M. Garcíaa, M. G. Corzoa, M. A. Domíngueza, M. A. Francob and J. M. Naharro, *J. Hazard. Mater.*, 2017, **328**, 46–55.
5 Y. C. Chang, S. W. Chang and D. H. Chen, *React. Funct. Polym.*, 2006, **66**, 335–341.
6 X. Zeng and E. Ruckenstein, *J. Membr. Sci.*, 1998, **148**, 195–205.
7 L. Lv, N. Chen, C. P. Feng, J. Zhang and M. Li, *RSC Adv.*, 2017, **7**, 27992–28000.
8 S. S. Ahluwalia and D. Goyal, *Eng. Life Sci.*, 2005, **5**, 158–162.
9 G. Aragay, J. Pons and A. Merkoçi, *Chem. Rev.*, 2011, **111**, 3433–3458.
10 D. G. Liu, Z. H. Li, W. Li, Z. G. Zhong, J. Q. Xu, J. J. Ren and Z. S. Ma, *Ind. Eng. Chem. Res.*, 2013, **52**, 11036–11044.
11 W. S. Wan Ngah and S. Fatinathan, *Chem. Eng. J.*, 2008, **143**, 62–72.
12 F. F. Menezes, F. R. H. de Silva, M. G. J. de Rocha and R. M. Filho, *Ind. Crops Prod.*, 2016, **94**, 463–470.
13 T. Tana, Z. Y. Zhang, L. Moghaddam, D. W. Rackemann, J. Rencoret, A. Gutiérrez, J. Del Río and W. O. S. Doherty, *ACS Sustainable Chem. Eng.*, 2016, **4**, 5483–5494.
14 X. Y. Guo, S. Z. Zhang and X. Q. Shan, *J. Hazard. Mater.*, 2008, **151**, 134–142.
15 Q. F. Lu, Z. K. Huang, B. Liu and X. S. Cheng, *Bioresour. Technol.*, 2011, **104**, 111–118.
16 X. H. Wang, Y. K. Zhang, C. Hao, X. H. Dai, Z. L. Zhou and N. C. Si, *RSC Adv.*, 2014, **4**, 28156–28164.
17 Y. M. Hao, M. Chen and Z. B. Hu, *J. Hazard. Mater.*, 2010, **184**, 392–399.
18 Y. S. Ho, *Water Res.*, 2003, **37**, 2323–2330.
19 S. M. Xu, S. Feng, F. Yue and J. D. Wang, *J. Appl. Polym. Sci.*, 2004, **92**, 728–732.
20 K. Kadirvelu, C. F. Brasquet and P. L. Cloirec, *Langmuir*, 2000, **16**, 8404–8409.
21 X. Luo, J. Zeng, S. Liu and L. Zhang, *Bioresour. Technol.*, 2015, **194**, 403–406.
22 R. H. Crist, J. R. Martin and D. R. Crist, *Environ. Sci. Technol.*, 2002, **36**, 1485–1490.

23 X. W. Peng, L. X. Zhong, J. L. Ren and R. C. Sun, *J. Agric. Food Chem.*, 2012, **60**, 3909–3916.
24 N. F. Ma, S. X. Chen, X. L. Liu and Y. Yang, *J. Appl. Polym. Sci.*, 2010, **117**, 2854–2861.
25 Y. Wu, S. Z. Zhang, X. Y. Guo and H. L. Huang, *Bioresour. Technol.*, 2008, **99**, 7709–7715.
26 Y. S. Ho and G. McKay, *Water Res.*, 2000, **34**, 735–742.
27 S. N. C. Ramos, A. L. P. Xavier, F. S. Teodoro, L. F. Gil and L. V. A. Gurgel, *Ind. Crops Prod.*, 2016, **79**, 116–130.
28 Q. Li, J. P. Zhai, W. Y. Zhang, M. M. Wan and J. Zhou, *J. Hazard. Mater.*, 2007, **141**, 163–167.
29 T. V. J. Charpentier, A. Neville, J. L. Lanigan, R. Barker, M. J. Smith and T. Richardson, *ACS Omega*, 2016, **1**, 77–83.
30 R. C. Sun, J. Tomkinson, X. F. Sun and N. J. Wang, *Polymer*, 2000, **41**, 8409–8417.
31 B. Rezaei, E. Sadeghi and S. Meghdadi, *J. Hazard. Mater.*, 2009, **168**, 787–792.
32 Y. Zhang, R. J. Qu, C. M. Sun, C. H. Wang, C. N. Ji, H. Chen and P. Yin, *Appl. Surf. Sci.*, 2009, **255**, 5818–5826.
33 K. Mandel, F. Hutter, C. Gellermann and G. Sextl, *ACS Appl. Mater. Interfaces*, 2012, **4**, 5633–5642.
34 K. Mandel, F. Hutter, C. Gellermann and G. Sextl, *ACS Appl. Mater. Interfaces*, 2012, **4**, 5633–5642.
35 H. Y. Yu, A. Fisher, D. J. Cheng and D. P. Cao, *ACS Appl. Mater. Interfaces*, 2016, **8**, 21431–21439.
36 S. Deng and Y. P. Ting, *Water Res.*, 2005, **39**, 2167–2177.
37 I. Platzman, R. Brener, H. Haick and R. Tannenbaum, *J. Phys. Chem. C*, 2008, **112**, 1101–1108.